New insights into biochar ammoniacal nitrogen adsorption and its correlation to aerobic degradation ammonia emissions

Matheus Vieira Firmino, Anne Tremier, Annabelle Couvert, Anthony Szymczyk

New insights into biochar ammoniacal nitrogen adsorption and its correlation to aerobic degradation ammonia emissions

Matheus Vieira Firmino[a*], Anne Trémier[a], Annabelle Couvert[b], Anthony Szymczyk[c]

[a] INRAE, OPAALE, F-35044, Rennes, France. Email addresses: matheus.vieira-firmino-silva@inrae.fr and anne.tremier@inrae.fr

[b] Univ Rennes, Ecole Nationale Supérieure de Chimie de Rennes, CNRS, ISCR - UMR 6226, F-35000 Rennes, France. Email address: annabelle.couvert@ensc-rennes.fr

[c] Univ Rennes, CNRS, ISCR (Institut des Sciences Chimiques de Rennes) – UMR 6226, Rennes, France. Email address: anthony.szymczyk@univ-rennes1.fr

*Corresponding author at: INRAE, OPAALE, F-35044, Rennes, France. E-mail address: matheus.vieira-firmino-silva@inrae.fr

Abstract

One of the technical barriers to the wider use of biochar in the composting practices is the lack of accurate quantification linking biochar properties to application outcomes. To address this issue, this paper investigates the use of ammonia nitrogen adsorption capacity by biochar as a predictor of ammonia emission during composting in the presence of biochar. With this in mind, this work investigated the use of ammonia nitrogen adsorption capacity of biochar when mixed with solid digestate, and the reduction in ammonia emissions resulting from the addition of biochar during aerobic degradation of solid digestate. A biochar synthesized at 900°C, another synthesized at 450°C, and two derivatives of the latter biochar, one chemically modified with nitric acid and the other with potassium hydroxide, were tested. This study concluded that the chemical characteristics of the biochar, including pH and oxygen/carbon

atomic ratio, had a greater influence on the adsorption of ammonia nitrogen than physical attributes such as specific surface area. In this regard, nitric acid modification had superior performance compared to hydroxide potassium modification to increase biochar chemical attributes and reduce ammonia emissions when applied to aerobic degradation. Finally, a significant linear correlation (p-value < 0.05, r^2 = 0.79) was found between biochar ammonia nitrogen adsorption capacity and ammonia emissions along composting, showing the potential of this variable as a predictive parameter. This study provides insights for future explorations aiming to develop predictive tests for biochar performance.

Abbreviations

ANOVA = analysis of variance

AW = solid digestat issued from mix of agricultural and agro-industrial wastes

BC = biochar

BC_C = biochar distributed by a commercial company

BC_C_HNO3 = BC_C modified with HNO3

BC450 = biochar produced at 400-450°C

BC450_HNO3 = BC450 modified with HNO3

BC450_KOH = BC450 modified with KOH

BC900 = biochar produced at 700-900°C

CV = coefficient of variation

DM = dry matter

FTIR = Fourier transform infrared spectroscopy

FW = fresh weight

HNO_3 = nitric acid

KCl = potassium chloride

KOH = potassium hydroxide

n = number of observation

N_2 = atmospheric nitrogen

N_2O = nitrous oxide

NA = not available

ND = not detected

NH_3 = ammoniac

$NH3_e$ = NH3 emissions

NH3er = NH3 emissions reduction compared to control

NH_4^+ = ammonium

$N\text{-}NH_4^+$ = ammoniacal nitrogen, defined as the sum of nitrogen in the form of ammonia and ammonium in a sample.

OFMSW = solid digestat issued from organic fraction of municipal solid waste

r = Pearson correlation coefficient

SD = standard deviation

TKN = total Kjeldahl nitrogen

VS = volatile solids

1 Introduction

Composting is a biological aerobic process used for treating a large variety of organic wastes, from animal manures to industrial residues (Gajalakshmi and Abbasi, 2008). This process changes the organic waste's properties through a reduction in moisture, pathogens inactivation, stabilization of organic matter and synthesis of humic substances, leading to a high-value material for soil application (Haug, 1993). Despite these benefits, composting generates environmental impacts, notably through nitrogen emissions. Indeed, along the composting treatment the organic nitrogen can be mineralized to its ammonia (NH_3) form and then stripped out of the composting medium. These NH_3 emissions are generated by the displacement of the equilibrium NH_4^+/NH_3 to the gaseous form and favoured by the composting medium aeration supplied either by forced aeration (generally air blowing) or turning operations (de Guardia et al., 2010). The inherent composting conditions, such as high temperature (>40°C), and the organic waste's properties, such as high pH (>8), contribute to NH_3 production (Sanchez-Monedero et al., 2018). Thus, NH_3 emissions are an inevitable aerobic degradation characteristic. On the other hand, the nitrification/denitrification microbiological process generates nitrous oxide (N_2O) and atmospheric nitrogen (N_2). Along composting, nitrification occurs through the oxidation of ammonium (NH_4^+) by ammonia-oxidizing bacteria and archaea, which generates hydroxylamine (NH_2OH), nitrite (NO_2^-) and nitrate (NO_3^-) anions (Zeng et al., 2013). These oxidized nitrogen forms can be transported to micro spots of anoxic environment, favouring the development of anaerobic microorganisms that use oxidized nitrogen as their final electron acceptor and produce N_2O and N_2 (Cáceres et al., 2018). These nitrogen losses occur mainly as gaseous emissions in the form of NH_3, N_2O and N_2, contributing to environmental problems such as acid rain (Leip et al., 2015), the formation of fine particles and global warming (Sekar et al., 2021)

Different strategies have been investigated to reduce nitrogen emissions, such as finding optimal operational conditions, such as aeration, or the use of various bulking agents. In recent years, supplementing the composting mixture with biochar (BC), i.e. chars intended for environmental applications, has proven to be a promising strategy to capture nitrogen in composts. The literature reports nitrogen losses and NH_3 emission reductions of 6-86% and 7-98%, respectively (Sanchez-Monedero et al., 2018).

Despite these advantages and more than ten years of research into the addition of biochar during composting, its use in composting practices has not yet been adopted. An important obstacle to biochar broader utilization lies in the absence of precise quantification linking biochar properties to application outcomes (Hu et al., 2021). This deficiency undermines buyers confidence in the investment made through the purchase of biochar, emphasizing the need for a clearer understanding of its effects in order to build trust in its application. In addition, the characteristics of biochar vary considerably (Vieira Firmino, M., Trémier, 2023), because of the heterogeneity of feedstock (Zhao et al., 2013), as well as pyrolysis operational parameters such as heating temperature and holding time (Shaaban et al., 2014). The heterogeneity of the final product can be an obstacle for biochar suppliers who wish to guarantee uniform and consistent results from biochar application. The development of a straightforward test that empower biochar users to anticipate its effects before incorporating it into composting processes might ease its adoption.

To develop such a test, it is first necessary to identify the pertinent biochar effect to be predicted. Within the context of biochar application in composting, a primary focus is on its ability to mitigate nitrogen losses, given its significant environmental and agronomic implications. Ammonia emissions is the main pathway of nitrogen losses in composting (Pardo

et al., 2015). Consequently, it was judge pertinent to selected NH_3 emissions as the parameter to be predicted in the development of the test.

To identify viable strategies for developing a prediction test for NH_3 emissions, the current mechanistic understanding of biochar's impact on the nitrogen cycle in composting was accessed. Various authors have attributed the reduction in nitrogen losses with biochar amendment to its adsorption capacities. In this regard, Joseph et al. (2018) hypothesized that when a biochar is mixed with organic wastes, it adsorbs moisture with dissolved inorganic nitrogen, especially NH_4^+, before its surface is covered with soluble carbon. Subsequently, microbiological or chemical reactions could oxidize the trapped NH_4^+. In this way, biochar would reduce the amount of free NH_4^+, which could otherwise be volatilized as NH_3. In addition, there are indirect benefits associated with the adsorption of NH_4^+ by biochar. Indeed, the high concentration of ammonium in some organic wastes such as digestate (Manu et al., 2021) can be toxic to nitrifying microorganism (Cáceres et al., 2018). Thus, the adsorption of NH_4^+ onto biochar would create a better environment for nitrification (Li et al., 2023), that also leads to a reduction of NH_4^+ available for volatilization. As so, $N\text{-}NH_4^+$ adsorption on biochar has often been suggested to be related to NH_3 emissions reduction in aerobic degradation (Agyarko-Mintah et al., 2017; Li et al., 2023; Steiner et al., 2010).

Based in these results, it is plausible to hypothesize that a significant statistical correlation might exist between biochar adsorption of ammoniacal nitrogen in compost and its capacity to reduce NH_3 emissions. Consequently, estimating biochar's adsorption of ammoniacal nitrogen in compost could serve as a reliable predictor of its capability to reduce NH_3 emissions. However, the capacity of biochar to adsorb ammoniacal nitrogen ($N\text{-}NH_4^+$), i.e. the sum of nitrogen in the form of ammonia and ammonium in a sample, in a solid environment has

rarely been estimated and the statistical correlation between N-NH_4^+ adsorption and the reduction of ammonia emissions has not been demonstrated. Indeed, the works available in the literature dealing with the capacity of biochar to adsorb NH_4^+ mainly present adsorption results in liquid solution using isothermal models (Zhang et al., 2020). To our knowledge, no work has yet attempted to estimate and optimize the potential of biochar to adsorb N-NH_4^+ in solid organic waste. Yet, solid organic waste represents a complex environment with varying moisture content and heterogeneous chemical concentrations, soluble organic matter and biological activity that could make previous models inaccurate.

Moreover, the confirmation of the correlation between N-NH_4^+ adsorption onto biochar and the reduction of NH_3 emissions during composting with biochar demands testing biochars with diverse N-NH_4^+ adsorption capacities. In this regard, biochar chemical modifications could be a helpful tool. Biochar modifications aim to increase properties usually related to adsorption, such as surface area, ion exchange capacity and surface functional groups. Literature reviews show that, in liquid solutions, modified biochar can adsorb more N-NH_4^+ (mean = 22.79 mgN.gBC^{-1}, number of observations = 12) than unmodified ones (mean = 11.9 mgN.gBC^{-1}, number of observations = 65) (Zhang et al., 2020). It would thus be interesting to apply this approach to N-NH_4^+ adsorption on biochar in solid organic waste. Closer investigation of the different modifications available shows that nitric acid (HNO_3) and potassium hydroxide (KOH) modifications are interesting alternatives. It was reported that HNO_3 and KOH modifications increased biochar NH_4^+ adsorption capacity by 36% (Vu et al., 2017) and 39% (Song et al., 2020),compared to the unmodified biochar, when tested in 40 and 10 mgNH_4^+.L^{-1} solutions, respectively. Vu et al. (2017) suggested that the HNO_3 modification improves NH_4^+ adsorption by increasing biochar surface chemical groups and total acidity, while Song et al. (2020) attributed KOH modification efficiency to an increase in

158 biochar surface area and pore structure. These results suggest that physical and chemical
159 adsorption mechanisms co-exist in biochar, as shown by Song et al. (2020) who studied
160 biochar NH_4^+ adsorption in wastewater. Some authors highlighted that chemical
161 characteristics such as cation exchange capacity and surface acidity (Gai et al., 2014; Yang et
162 al., 2018) had higher influence over biochar NH_4^+ adsorption in wastewater than the surface
163 area (Takaya et al., 2016). Thus, it is essential to understand which biochar's characteristics
164 are related to its capacity to adsorb N-NH_4^+ in organic waste in order to identify the main
165 reactional mechanisms and optimize biochar production for supplementation of organic
166 waste composting.

167 In this context, the present work had three objectives. Firstly, to investigate whether there is
168 a statistically significant correlation between the ammoniacal nitrogen of biochar in organic
169 waste and its ability to reduce NH_3 emissions. In addition, this work assesses whether the
170 chemical modifications of biochar KOH and HNO_3 can improve the potential of biochar to
171 reduce NH_3 emissions during aerobic degradation. Finally, this work seeks to identify the main
172 characteristics of biochar linked to the adsorption of ammoniacal nitrogen in organic waste
173 and to NH_3 emissions.

174 2 Materials and methods

175 2.1 Studied substrates

176 Solid digestates, which are residues of anaerobic digestion, were studied in this work because
177 one of their characteristics is the high content in N-NH_4^+. Two types of digestate were used.
178 The first one was produced from the anaerobic digestion of a mix of agricultural and agro-
179 industrial wastes (AW), such as cattle manure (20t) and slurry (20t) and cheese whey (12t).
180 The complete list of organic wastes used in AW production is available in Supplementary

Materials. The second one was collected in an industrial anaerobic digestion plant treating sorted organic fraction of municipal solid waste (OFMSW). In both cases, the solid digestate was collected directly after solid/liquid separation by a screw press, and it was stored at -20°C to preserve its chemical characteristics.

Three biochars were considered in this study. Two of these were produced in a rotary kiln 4.2 m long and 0.2 m in diameter using green waste pallets made from beech branches. Pyrolysis was carried out with a biomass feed rate of 6 kg.h-1, a rotation speed of 3 RPM, an inclination of 3°, an incoming nitrogen flow of 4 NL.min-1, and a residence time of 40 minutes. Two temperatures of pyrolysis were considered: one biochar was produced in a low temperature range, 400-450°C (BC450), and a second at high temperature range, 700-900°C (BC900). The kiln was fed with 6kg.h^{-1} of biomass and had a residence time of 40 minutes. The third biochar is a retail biochar (5kg) distributed by a commercial company (BC_C).

2.2 Biochar modifications

In order to increase the diversity of properties of the studied biochar, the raw biochars presented above have been subjected to chemical modifications. A preliminary study was carried out to select the most relevant chemical modifications (data not shown). In this study, all biochars were subjected to modifications using HNO_3, KOH, H2SO4 and HCl. The modifications that induced the most significant changes in the infrared spectra of the biochars were selected for the present work. In this regard, an acid modification (HNO_3) was used to activate BC450 and BC_C, generating BC450_HNO_3 and BC_C_HNO_3. Moreover, BC450 was also activated using a basic attack (KOH), generating a third modified biochar (BC450_KOH). These modifications were based on Song et al. (2020) and Shang et al. (2018) works. Previous

experiments (data not presented) showed that BC900 chemical and physical properties cannot be altered by any of the tested modifications.

The acid and basic activations consisted in soaking the biochars, at room temperature and under constant agitation, into a 6 or 3 mol.l^{-1} HNO_3 or KOH solution for 16 or 24h at 1:10 or 1:20 ratio (mass of biochar/volume of reactant solution) respectively. Afterward, the soaked biochar was washed until the washing solution achieve pH close to neutral. Biochars were then dried at 105°C for 24h and stored in closed opaque recipients and at ambient temperature.

2.3 Measurement of biochar capacity to adsorb NH_4^+

Biochar was mixed with AW or OFMSW at 10% biochar to digestate ratio (fresh weight) in a 250ml beaker for 48h at room temperature. The beakers were sealed with Teflon to avoid NH_3 volatilization and drying. The contact period of 48h was chosen based on the work reported by Prost et al. (2013). The authors showed that pores of biochar mixed with farmyard manure clogged with dissolved organic matter after two days, preventing major adsorption after this date.

After 48h, the biochar granules were separated from the digestate using tweezer and the solid digestate fibers and debris attached to the biochar particles were manually removed. The adsorbed NH_4^+ was then extracted based on the norm NF ISO 14.256-2. The extractions consisted in soaking the biochar granules in 1M potassium chloride (KCl) solution for 1h under constant agitation at ambient temperature. Afterwards, the soaked biochar was separated by centrifugation at 12000 rpm. The extracted solution was filtered through a 0.45µm polypropylene filter with glass fibber. The NH_4^+ content of the solution was then measured by ionic chromatography using Metrohm 850 Professional IC.

This procedure was applied to BC450, BC450_KOH, BC450_HNO_3 and BC900 in quadruplicate, but not to BC_C and BC_C_HNO_3. Indeed, the granulometry (powder) of these latter biochars prevented their use in this test.

2.4 Aerobic degradation test

The influence of biochar properties over NH_3 emission reduction during aerobic degradation was tested using mixtures of digestate AW and biochar with a biochar to digestate ratio of 5% (wet weight).

To perform aerobic degradation, a pilot composed of six 10 L stainless steel reactors was used. The reactors are operated with controlled temperature (40°C) and aeration (70 $L.h^{-1}$). Part of the reactor outlet gas recirculates in the system to allow the homogenization of the air within the reacting cell. The recirculation airflow was set to approximately 5 $L.min^{-1}$. The composition of the inlet and outlet gas was analysed using an inline analyser ABB EL3020 that measures the concentration of carbon dioxide (CO_2), oxygen (O_2), methane (CH_4) and nitrous oxide (N_2O). In addition, the NH_3 emitted by the cells was quantified in a parallel circuit containing two ammonia traps with 200 mL of sulphuric acid 1M. The ammonia traps were analysed by distillation in a Gerhardt vapodest 50. The aerobic degradation device and operational conditions were similar to those of Berthe et al. (2007) and Zeng et al. (2013). The complete scheme of the aerobic degradation pilot can be visualized in Supplementary Materials.

Each experiments lasted two weeks.

2.5 Digestates characterization

Analyses of the digestates included the determination of total Kjeldahl nitrogen (TKN), total N-NH_4^+, easily extractable N-NH_4^+, dry matter (DM), volatile solids (VS) and pH. The dry matter (DM) was obtained by drying the sample at 105°C for 48h, and the volatile solids (VS)

concentration by loss-on-ignition at 550°C for 5h. The total Kjeldahl nitrogen (TKN) was determined by distillation in a Gerhardt Vapodest 50 after sample mineralization with sulphuric acid 98% (v:v) and copper tablets in a Mineralization Bloc Kjeldatherm KT followed, according to the norm NF EN 13342.

The total ammoniacal nitrogen content was determined in Büchi distillation Unit K-350. To perform Büchi distillation, samples were basified with magnesium hydroxide right before being inserted into the device. The distillation was performed with water vapour for approximately 3 minutes. Easily extractable ammoniacal nitrogen was calculated through 1M KCl extraction at 1:10 (w:w, wet weight) ratio during 1h. The extracted solution was filtered through a 0.45 µm polypropylene filter with glass fibber and analysed using Metrohm 850 Professional ionic chromatography. It is expected that the harsher extraction conditions used in Büchi distillation compared to KCl extractions, might estimate the total N-NH_4^+. At the same time, it is expected that KCl extractions would estimate the more labile fraction of total N-NH_4^+.

The pH was measured by mixing the digestate with deionised water in a ratio of 1:5 (w:w, wet weight) and stirring for 1 hour, in accordance with standard NF EN 13037. Afterwards, the pH was measured using Mettler Toledo Five Easy. All previous mentioned analyses were performed in triplicate (if not attested otherwise), except for ammonia traps which were analysed in duplicate. The ammonia traps samples were homogeneous, and the individual analyses differed less than 0.5% from the mean.

2.6 Biochar characterization

Biochars were characterized for TKN, DM, VS and pH using the same methodology applied to digestates. In addition, biochar's elemental composition (carbon, nitrogen, sulfur and

oxygen), surface area, Fourier transform infrared spectroscopy (FTIR) and zeta potential were analysed. The elemental analysis was performed using an elemental analyser flash 2000. Additionally, the total oxygen and total carbon results from the elemental analysis were converted to number of atoms and the atomic ratio TO/TC was calculated. The specific surface area was determined using a Micromeritics 3Flex analyser with nitrogen as the adsorbent gas and applying the model Brunauer-Emmett-Teller (BET).. The FTIR analysis was done in the wavelength's region from 4000 to 400 cm^{-1} with a spectral resolution of 4 cm^{-1} using a Nicolet iS5 with ATR iD7 module.

Biochar zeta potential was inferred from streaming potential measurement, which is a versatile technique for characterizing the electrical surface properties of materials of different geometries such as polymer films (Szymczyk et al., 2007), porous materials (Fievet et al., 2004) or particles (Szymczyk et al., 2002). Experiments were carried out with a SurPASS electrokinetic analyser (Anton Paar GmbH). A porous plug was formed with biochar particles of millimetric dimensions. It was further surrounded by two Ag/AgCl flow electrodes allowing circulation of the measuring solution (0.001 M KCl) between the particles and measurement of the streaming potential generated by the application of pressure ramps (0-300 mbar) through the porous plug. All experiments were performed at T = 20 ± 2 °C and duplicated. The pH of the measuring solution was adjusted with 0.05 M HCl and KOH solutions. The zeta potential (ζ) of biochars was determined from experimental streaming potential (ΔV_s) values from the well-known Helmholtz-Smoluchowski expressed as:

$$\zeta = \frac{\Delta V_s \eta \lambda_0}{\varepsilon_0 \varepsilon_r \Delta P} \quad (1)$$

Where η is the viscosity of the measuring solution, λ_0 its electric conductivity, ε_r its dielectric constant, ε_0 is the vacuum dielectric permittivity and ΔP is the hydrostatic pressure difference applied through the porous plug formed by the biochar particles.

Some biochars were found to release colloidal particles (generated during the pyrolysis process or post modifications (Yang et al., 2020) into the measuring solution during streaming potential experiments. The zeta potential of these particles was determined from their electrophoretic mobility measured by electrophoretic light scattering (Wallis zeta potential analyzer, Cordouan Technologies), considering the Smoluchowski equation for electrophoretic mobility (u_E):

$$\zeta = \frac{u_E \eta}{\varepsilon_0 \varepsilon_r} \qquad (2)$$

Where η is the viscosity of the measuring solution, ε_r its dielectric constant, ε_0 is the vacuum dielectric permittivity.

2.7 Data analysis

At the end of the adsorption tests, the influence of digestate type (AW or OFMSW), biochar type (BC450, BC450_HNO_3, BC450_KOH, BC900) over biochar N-NH_4^+ adsorption was studied using one-way and two-way ANOVA. The differences in biochar N-NH_4^+ adsorption capacity obtained in the adsorption tests and the differences in aerobic degradation NH_3 emissions were investigated using two tailed welch t-test.

To compare nitrogen losses from different reactors, the NH_3 emissions (NH_{3e}) and NH_3 emissions reductions (NH_{3er}) were defined according to:

$$NH_{3e} = \frac{NH_{3\ stripped} \cdot 100}{TKN_i} \quad (3a)$$

$$NH_{3\ er} = \frac{(NH_{3c} - NH_{3bc}) \cdot 100}{NH_{3c}} \quad (3b)$$

Where TKN_i is the Total TKN initially present in the cell, NH_3 stripped is the NH_3 captured in acid traps, NH_{3C} is the NH_3 emissions in control (%), NH_{3BC} is the NH_3 emissions in biochar treatment (%), NH_{3e} is the NH_3 emissions and NH_{3er} is the NH_3 emissions reduction.

Furthermore, the influence of biochar $N\text{-}NH_4^+$ adsorption (e.g. estimated by the adsorption tests) over aerobic degradation NH_3 emissions (e.g. estimated through aerobic degradation tests) was estimated using a Pearson correlation and linear regression. Additionally, the investigation of biochar characteristics related to biochar NH_4^+ adsorption and aerobic degradation NH_{3er} was done using a Pearson Correlation Matrix.

The confidence level of all statistical analysis was defined at 90%. All statistical analyses were done using the software R Studio version 3.5.1.

3 Results and Discussion

3.1 Substrates characteristics

The substrate characteristics are presented in Table 1.

Table 1. Physicochemical characterization of substrates

Analysis with less than three repetitions had all their values showed in the table.

Studied digestates differed in their nitrogen composition. Digestate AW had higher TKN and total $N\text{-}NH_4^+$ than OFMSW. Results show that AW TKN is composed of a higher proportion of $N\text{-}NH_4^+$ (45.6%) compared to OFMSW (37.5%). In addition, Table 1 shows that the values of

335 total N-NH_4^+ and easily extractable N-NH_4^+. AW had higher total N-NH_4^+ but lower easily
336 extractable N-NH_4^+ compared to OFMSW. Thus, it is likely that AW N-NH_4^+ is more linked to
337 the organic matter structure than OFMSW N-NH_4^+.

338 The analysis of biochar characteristics, presented in table 1, shows that the higher
339 temperature used for the production of the BC900 contributes to degrade more OM during
340 pyrolysis, consequently creating a larger amount of ashes, a lower percentage of oxygen, a
341 higher percentage of carbon and a higher specific surface area compared to BC450. Similar
342 results were reported in the literature (Shaaban et al., 2014; Tag et al., 2016). BC_C had an
343 elemental composition (TC, TH, TN and TO) and pH similar to BC900 (Table 1), suggesting that
344 similar pyrolysis conditions might have been employed in its production.

345 The chemical reactions applied to biochars effectively changed BC450 and BC_C chemical
346 characteristics. Chemical modifications (HNO_3 and KOH) reduced the ash contents compared
347 to the original biochars, generating an increase in the proportion of VM (Table 1). The
348 reduction in ash content might have contributed to decrease biochar pH. Moreover, Table 1
349 shows that KOH modification had small impact over BC450 elemental analysis and surface
350 area. The KOH modification applied in this study differed from the one presented in the
351 literature by avoiding catalysis step usually performed at high temperature (~500°C) and in
352 an oxygen-limited environment (Ma et al., 2022; Song et al., 2020). The lack of a catalysis step
353 in this study might have limited the effect of KOH modification.

354 The pH analysis of biochars (Table 1) shows that BC900 and BC_C had the highest pH with
355 values close to 9. The lack of acid groups and the ashes content might have contributed to
356 this result. Additionally, BC450_KOH reduced BC450 pH from 6.7 to 5.5. This result could be
357 due to a reduction in ash content or functionalization of biochar surface. In addition, the HNO_3

modifications reduced the pH of the biochar to 2.5 and 3.0 for BC450_$HN0_3$ and BC_C_HNO_3 respectively. Yakout (2015) reported similar results concerning HNO_3 modifications. The authors modified rice straw with 65% nitric acid at 60°C. The modification reduced biochar pH to values ranging from 3.4 to 3.2, while the non-modified biochar had pH close to 9. The pH is affected by the deprotonation of acid and basic groups on the biochar surface, in liquid. Thus, this analysis suggests that studied biochars differed by their surface functions.

The elemental analysis supports this idea. Table 1 shows that HNO_3 modification increased TO and TN and reduced TC and TH percentages when applied to BC450 or BC_C. These changes increased the atomic ratio TO/TC by 41% and 111% for BC450 and BC_C, respectively, suggesting that HNO_3 modification increased biochar oxidation (Wang et al., 2019). Similar results were reported by Shang et al. (2018). The authors modified spruce sawdust biochar produced at 400°C using 6M HNO_3 chemical modification. Their elemental analysis showed that HNO_3 modified biochar increased TO and TN in 7.4 and 3.3% compared to the original biochar. In addition, it has been shown that HNO_3 can functionalize the biochar surface (Mehmood et al., 2021; Shang et al., 2018), resulting in increased oxygen and nitrogen contents.

A more detailed analysis of biochar functionalization can be achieved through FTIR (Fig. 1).

Fig. 1. Fourier transform infrared spectra from (A) BC_C, BC_C_HNO_3 and BC900. (B) BC450, BC450_HNO_3 and BC450_KOH.

Fig. 1A firstly shows that BC900 and BC_C had similar FTIR spectra marked by the lack of detectable peaks. The similarity between both spectra reinforces the idea that these biochars had similar production conditions. Moreover, it can be assumed that BC900 high pyrolysis

temperature degraded the majority of surface chemical functions. This hypothesis could be verified by ATG-DSC analysis in future studies.

Contrastingly, FTIR spectrum obtained with BC450 (Fig. 1B) showed three identifiable peaks in the functional group region. The first peak at 3000-2800 cm^{-1} is attributed to the asymmetric and symmetric C−H stretching vibrations of the methyl (−CH_3−) and methylene (−CH_2−) (Vu et al., 2018). The second peak close to 1700 cm^{-1} is attributed to carboxylic and lactonic groups (C═O) (Tran et al., 2018; Vu et al., 2018). Lastly, the peak close to 1650 cm^{-1} is attributed to (C═C) double bonds in aromatic rings (Tran et al., 2018; Vu et al., 2018).

Additionally, BC450_KOH FTIR spectrum was not notably different from the spectrum obtained with BC450 concerning the previous described peaks. On the other hand, BC450_HNO_3 reduced the methyl (−CH_3−) and methylene (−CH_2−) peak and increased carboxylic and lactonic peak, compared to BC450. Furthermore, the HNO_3 modification applied to BC_C generated a detectable but minor change on the carboxylic and lactonic peak. Vu et al. (2018) reported similar results. The authors modified corncob biochar with 4M HNO_3 and observed the appearance of a FTIR peak at 1705 cm^{-1}, which was attributed to carboxylic acid. The FTIR reinforces the conclusion of the elemental and pH analyses, suggesting that modification with HNO_3 increases the acid groups on the biochar surface.

Since these acid groups can deprotonate, their presence can also be revealed by determining the zeta potential of biochars. Fig. 2 indeed shows that biochars are negatively charged over the whole pH range considered in the streaming potential experiments.

Fig. 2. Zeta potential of BC450, BC450_KOH, BC450_HNO_3 and BC900 inferred from streaming potential measurements vs. pH.

By definition, the isoelectric point is the pH at which a particle carries no net electrical charge, and consequently, its zeta potential is zero (Sujith et al., 2022). Moreover, a decrease in pH favours the protonation of acid groups, reducing the particle's electronegativity and increasing the zeta potential. Considering that no biochar has reached its isoelectric point at pH 3, it can be concluded that a lower pH would be required to achieve this. This result is in good agreement with data reported in the recent review article published by Yang et al. (2020).

According to Fig. 2, the BC900 was less charged than BC450 and BC450_KOH, whatever the pH of the measuring solution. This result is due to the higher pyrolysis temperature used to produce BC900, which reduced the density of surface acid groups (Shaaban et al., 2014; Yang et al., 2020). Thus, zeta potential values corroborate FTIR results. It can be noted, however, that zeta potential analysis indicates that the surface of BC450_KOH was more negatively charged than BC450 while FTIR did not show major differences between these two biochars.

Surprisingly, it was found that the zeta potential of BC450_HNO_3 decreased (in absolute value) with increasing pH (except for pH below 3.2). Although this behaviour can be explained in some cases by an increase in the electrical conductivity of the solution, this is only expected at very high pH values (Mouhoumed et al., 2014), which was not the case in the present work. This behaviour has already been reported in the literature and attributed to swelling effects with pH (Luxbacher and GmbH, 2014), which conceptually would be equivalent to a shift of the hydrodynamic slip plane with pH (Uetani and Yano, 2012). In this case, the concept of zeta potential loses its meaning. Indeed, during the electrokinetic titrations BC450_HNO_3 particles tended to partially disaggregate and colloidal particles were released into the measuring solution during streaming potential measurements. The zeta potential of a sample of the

426 solution containing colloidal particles from BC450_HNO_3 was determined by electrophoretic
427 light scattering. A value of -35.4 ± 1.6 mV was obtained at pH 3.5, which was higher (in
428 absolute value) than the one measured on all biochars. Colloidal biochar particles are
429 expected to bear the same chemical groups as bulk biochar (Yang et al., 2020) as confirmed
430 by measurements made on colloidal particles released by BC450. Indeed, electrophoretic light
431 scattering measurements led to a zeta potential value of -19.3 ± 3.1 mV at pH 3.5, which is in
432 good agreement with the streaming potential results reported in Fig. 2 (it is worth mentioning
433 that no colloidal particles were detected in the solutions used to characterize BC450_KOH
434 and BC900). Considering the colloidal biochar zeta potential as an estimation of the bulk
435 biochar zeta potential, it is possible to affirm that these additional electrophoretic light
436 scattering results suggest that BC450_HNO_3 was more (negatively) charged than the other
437 three biochars and that HNO_3 modification increased the amount of acid groups in BC450.
438 Similar results were reported by (Wang et al., 2019). The authors modified pinewood biochar
439 produced at 300 and 600°C with HNO_3 and pulverized the chars to study its colloidal
440 properties. It was reported that HNO_3 reduced zeta potential in approximately 6 mV. This
441 result was attributed to an increase in negatively charged oxygen-containing functional
442 groups.

443 Based on the previous analysis, it is possible to affirm that the initial biochars chosen for the
444 present study and the ones obtained after chemical modifications have high variability in their
445 chemical characteristics. They are thus expected to generate different N-NH_4^+ adsorption and
446 NH_3 loss quantities during their utilization with solid digestate.

3.2 Ammoniacal nitrogen adsorption capacity of biochar in a solid digestate environment

The results from biochar adsorption capacity when mixed to solid digestate are presented on Fig. 3.

Fig. 3. Ammoniacal nitrogen adsorbed in different biochars when applied to digestate made from agricultural wastes (AW) or digestate made from organic fraction of municipal solid waste (OFMSW).

A two-way ANOVA was conducted to examine the influence of biochar and digestate type on N-NH_4^+ adsorption. A statistically significant interaction was found between biochar type and digestate ($F(3,24) = 5.46$, p-value = 0.005, $\eta^2_g = 0.41$), indicating that the outcome of biochar N-NH_4^+ adsorption capacity depends not only on biochar properties, but also on digestate characteristics. Therefore, the analysis of the simple main effects (biochar and digestate type) was studied individually.

A one-way ANOVA was conducted to study how digestate type influenced each biochar adsorption capacity individually. This analysis shows that there is a significant difference (p-value < 0.1) between the amounts of N-NH_4^+ adsorbed by the biochars depending on whether they are applied to AW or OFMSW. A pairwise t-test analysis shows that all biochars had significant difference (p-value < 0.1) in their mean N-NH_4^+ adsorption whether applied to AW or OFMSW. On this subject, BC450_KOH, BC450_HNO_3, BC450 and BC900 adsorbed 41, 34 and 21 more N-NH_4^+ when applied to OFMSW compared to AW, respectively.

The higher biochar N-NH_4^+ adsorption when applied to OFMSW might be explained by the digestates chemical characteristics. Table 1 shows that OFMSW had higher easily extractable N-NH_4^+ (mean = 6.02 gN-NH_4^+.$kgDM^-$) compared to AW (mean = 4.62 gN-NH_4^+.$kgDM^{-1}$) whereas an opposite tendency is observed for the total N-NH_4^+ (e.g. 9.16 gN-NH_4^+.$kgDM^{-1}$ and

11.45 gN-NH_4^+.kgDM^{-1}, respectively). These results show that the easily extractable N-NH_4^+ is a good estimator of the organic waste N-NH_4^+ available to be adsorbed by biochar. Thus, the differences in N-NH_4^+ mobility in the organic waste structure may play an important role in biochar adsorption performance. It is likely that water mobility analysis with a method such as fast field cycling nuclear magnetic resonance relaxometry, might help to better understand the factors affecting biochar N-NH_4^+ adsorption.

The differences between biochars capacities to adsorb NH_4^+ were studied for each digestate individually (AW or OFMSW) using a one-way ANOVA. The results show that biochar type had a significant effect over N-NH_4^+ adsorption whether applied to AW ($F(3, 12) = 313$, p-value = $1.17e^{-11}$, $\eta^2_g = 0.99$) or OFMSW ($F(3, 12) = 96$, p-value = $1.15e^{-8}$, $\eta^2_g = 0.96$). A more in-depth analysis was done by calculating all pairwise comparisons between the different biochars (BC450, BC450_HNO_3, BC450_KOH and BC900) using a hypothesis test (T-Test). The results showed that the N-NH_4^+ adsorption was significantly different (p-value adjusted < 0.1) for all biochars (Fig. 3).

Biochar BC900 adsorbed the lowest amount of N-NH_4^+, with mean adsorption of 0.32 and 0.41 mgN-NH_4^+.gBC^{-1} when applied to AW and OFMSW, respectively. The higher BC900 surface area compared to other biochars suggested a better BC900 performance than the one observed. Surface area is considered as a critical parameter for adsorption because it relates to the density of the adsorption site per unity of mass (Zhang et al., 2020). In spite of its higher surface area, BC900 was not characterized by a higher density of adsorption sites, compared to other biochars, due to its considerably lower surface acid functions. This fact might justify its lower N-NH_4^+ performance.

Moreover, the hypothesis test results show that chemical activations applied to BC450 significantly increased the quantity of adsorbed N-NH_4^+. In this regard, BC450_HNO_3 and BC450_KOH respectively increased NH_4^+ adsorption by 514 and 577%, and 99 and 137% compared to BC450, applied to AW or OFMSW. Thus, it shows that the acid modification had superior performances to increase biochar N-NH_4^+ adsorption. These results evidence the importance of biochar chemical characteristics over N-NH_4^+ adsorption.

Furthermore, to optimize biochar N-NH_4^+ adsorption capacity, it is first necessary to identify the physicochemical properties related to this phenomenon. To answer this question, a Pearson correlation matrix was generated between biochar N-NH_4^+ adsorption capacity and biochar characteristics (Table 2).

Table 2. Pearson correlation results between NH_3 emissions, biochar N-NH_4^+ adsorption and biochar characteristics

BC sorp. = biochar N-NH_4^+ adsorption, n = number of observations, BC = biochar, TC = total carbon, TH = total hydrogen, TN = total nitrogen, TO = total oxygen, elemental analysis expressed as mass percentage in dry weight, SA = surface area, DM = dry matter, FM = fresh matter. '*' represent significant correlations (p-value < 0.1).

Table 2 shows significant correlations between biochar N-NH_4^+ adsorption and biochar pH, TN and the Atomic ratio TO/TC. These correlations suggest that biochar chemical characteristics plays an important role in N-NH_4^+ adsorption during solid digestate aerobic degradation. A more in-depth analysis, shows that lower pH biochars tend to have higher N-NH_4^+ adsorption capacity, probably thanks to its higher amount of negative surface charges generated by higher proportion of acid surface functions (as discussed in sections 3.1). This result is supported by the TO/TC atomic ratio, which is consider as an indicator of the density of acid functions in biochar. Thus, biochars with higher density of oxygen are more likely to adsorb more N-NH_4^+ during solid digestate aerobic degradation.

Interestingly, no significant correlation between biochar surface area and biochar N-NH_4^+ adsorption was found. This correlation was expected because higher surface area usually increases materials' adsorption capacity by increasing their density of adsorption sites per unit of mass (Zhang et al., 2020), which should reduce NH_3 emissions according to TO/TC correlation results. However, Table 1 shows that the biochar presenting higher surface area has the lower TO/TC atomic ratio. Previous discussion identified the increase in pyrolysis temperature as the cause of these changes (section 3.1). Thus, it is suggested that biochar surface area, and likely other physical characteristics, can have a role in NH_3 loss reduction, but they are not the primary determinant parameter.

Similar results have been reported in studies investigating biochar N-NH_4^+ adsorption in liquid solutions. Yang et al. (2018) and Takaya et al. (2016) found that biochars with higher surface areas (280-180 $m^2.g^{-1}$) did not had better capacities to adsorb N-NH_4^+ in liquid solution than lower surface biochars (<10$m^2.g^{-1}$). Furthermore, Yang et al., (2018) results shows that biochars with higher O/C ratio (i.e. 0.32) had higher NH_4^+ adsorption capacity (i.e. 5.38 $mg.g^{-1}$) compared with biochars with lower O/C ratios (i.e. 0.08). The authors highlighted the importance of electrostatic interactions (Yang et al., 2018) and chemical reaction with oxygen containing functional groups (Takaya et al., 2016).

Based on these results, it is possible to hypothesize that N-NH_4^+ adsorption by biochar in solid organic waste follows similar mechanisms to those observed in liquid solutions. However, further research is imperative to discern whether other specific mechanisms govern the N-NH_4^+ adsorption properties of biochar in solid organic waste.

3.3 Performance of ammoniacal nitrogen trapping by biochars in an aerobic degradation test

Aerobic degradation experiments were done using digestate AW and biochars BC450, BC450_KOH, BC450_HNO_3, and BC900 which adsorption capacity was previously estimated. In addition, BC_C and BC_C_HNO_3 were also tested, aiming to confirm the influence of HNO_3 modification over NH_3 emissions reduction during aerobic degradation.

3.3.1 Oxygen consumption and aeration

During aerobic degradation, experimental conditions such as aeration can greatly affect ammonia emissions (de Guardia et al., 2008). High aeration rates can lead to an increase in NH_3 emissions through stripping. On the other hand, low aeration rates can hinder oxygen availability in the reactors and slow down microbial metabolism, which can affect in return N-immobilization and ammonification. To ensure that the differences observed on NH_3 emissions during the experiments were only related to biochar adsorption, it was firstly necessary to investigate the impact of the aeration variations (measured through gas counters) on oxygen consumption, which is closely related to microbial metabolism during aerobic degradation. The mean aeration and total oxygen consumption are shown in Table 3.

Table 3. Aeration rate and oxygen consumption

VM_i = initial digestate volatile mater.

The results presented in Table 3 show that the aeration rate variability within the treatments was lower than 10.0%. Moreover, the whole treatment dataset presented a mean aeration of 69.2 $L.h^{-1}$ with a coefficient of variation of 6.2%. This low variation suggests that this factor did not had major influence over the results. An in-depth analysis of the results shows that one repetition from BC450_HNO_3 presented aeration rate of 58.98 $L.h^{-1}$, which was lower

than the dataset mean (69.2 $L.h^{-1}$) and lower than the other three repetitions values (e.g. 72.4, 73.4 and 72.7 $L.h^{-1}$). The anomalous aeration treatment here cited was taken into account in the following NH_3 emissions analysis.

Furthermore, the total oxygen consumption was analysed. A first observation shows that variability of results for each treatment condition was smaller than 5%, attesting the good repeatability of the experiment. In addition, the biochar effect over total oxygen consumption was investigated using pairwise t-test. No significant difference (p-value > 0.1) was found between control and biochar treatments. These results show that biochar supplementation did not influenced the aerobic biodegradability or microbial aerobic activity.

The previous analysis shows that operational parameters and composting microbial activity had small variability between the experiments, which means that differences in NH_{3e}, discussed in the next session, are likely related to biochar action.

3.3.2 Impact of biochar adsorption capacities over ammonia emissions during aerobic degradation

Fig. 4 presents the results of ammonia emissions depending on the type of added biochar.

Fig. 4. Ammonia emissions expressed as percentage of Total Kjeldahl Nitrogen. Ctrl = control treatment, without biochar (n = 3), BC450 (n = 3), BC450_KOH (n = 3), BC450_HNO_3 (n = 4), BC_C_HNO_3 (n = 2), BC900 (n = 2), BC_C (n = 3), n = number of observations. Red triangles indicate the treatments means.

A pairwise Welch t-test was conducted to study the differences between the experiments. The emissions of NH_3 measured in experiments with mixtures containing biochars BC450, BC450_HNO_3, BC_C_HNO_3 and BC900 were significantly different (p-value < 0.1) from those measured in the control experiment. The control emitted 21.0% (SD = 1.3) of its initial TKN as

583 NH_3, while the treatments BC450, BC450_HNO_3 and BC_C_HNO_3 reduced this value from
584 13.2%, 83.0% and 37.8%, respectively. On the other hand, BC900 increased NH_3 emissions
585 from 30.2% (SD = 1.9). Additionally, BC450_HNO_3 experiment with low aeration (previous
586 identified) did not affect the identification of the previous mentioned significant effect.
587 Finally, BC450_KOH and BC_C experiments did not significantly differ from the control.
588 Nevertheless Fig. 4. shows that one experiment of the BC450_KOH triplicate led to extremely
589 higher NH_3 emissions than the two others. This extreme point was the highest NH_3 emissions
590 observed during the experiments, achieving 36.7%. For comparison, the other two repetitions
591 had mean NH_3 emissions of 14.6%, and the mean of the whole experimental dataset was
592 18.1%. No apparent differences appeared in the experimental conditions between
593 BC450_KOH triplicates. However, digestate is a heterogeneous substrate, and the small
594 reactional volume (10 L) used increases the risks of having the results impacted by this
595 inherent digestate characteristic. The comparison between control NH_3 emissions and
596 BC450_KOH without this outlier point shows a significant difference (p-value = 0.049).

597 Moreover, the comparison between BC450 and its modifications shows that HNO_3 chemical
598 activation significantly reduced the NH_3 emissions by 80.4%. On the other hand, no significant
599 difference was found between BC450 and KOH modification, when considering the outlier
600 point. The efficiency of HNO_3 activation was confirmed by experiments with BC_C and
601 BC_C_HNO_3, where the modified biochar reduced NH_3 losses by 92% compared to BC_C.

602 The utilization of HNO_3 to augment biochar adsorption capacity of N-NH_4^+ has been
603 technically demonstrated in this study. However, it is important to highlight that a financial
604 study taking into account cost of production, agronomic benefits and composting market is
605 necessary before its industrial development can be considered. The analysis of biochar

properties revealed significant Pearson correlations (p-value < 0.05) between ammonia emissions and pH (r = -0.91) as well as the atomic ratio O/C (r = 0.81). Notably, no significant correlation was observed between ammonia emissions and biochar-specific surface area. Interestingly, similar correlations were identified between biochar properties and its $N\text{-}NH_4^+$ adsorption capacity, supporting the hypothesis that ammoniacal nitrogen adsorption is the primary factor influencing biochar's ability to mitigate NH_3 emissions. Furthermore, it is plausible that $N\text{-}NH_4^+$ adsorption by biochar particles contributes to the reduction in the size of the free ammoniacal nitrogen pool during the composting process. This reduction in NH_4^+ availability may subsequently limit the potential for NH_4^+ to be volatilized as NH_3, thereby contributing to the observed decrease in ammonia emissions. These findings underscore the intricate relationship between biochar properties, ammoniacal nitrogen adsorption, and their collective impact on reducing NH_3 emissions during composting.

Based on these results, it clearly appears that differences in biochar adsorption capacity led to a variation in biochar efficiency to reduce NH_3 emissions along aerobic degradation. To quantify the correlation between biochar adsorption potential and NH_3 emissions, a linear regression was thus calculated between NH_3 emissions (%TKNi) and biochar $N\text{-}NH_4^+$ adsorption potential ($gN\text{-}NH_4^+.kgBC^{-1}$). The results are presented in Fig 5.

Fig. 5. Linear regression between Biochar ammoniacal nitrogen adsorption and NH_3 emissions during aerobic biodegradation of AW. Vertical and horizontal bars represent the standard errors from NH_3 emissions and BC $N\text{-}NH_4^+$ adsorption, respectively. $NH_{3emissions} = -2.76.BC_{NNH4sorption} + 25.47$, $R^2 = 0.79$, p-value = 0.043. The complete linear regression table can be visualized in the Supplementary Materials.

The Fig. 5 shows a significant (p-value = 0.043) strong linear correlation ($R^2 = 0.79$) between both variables. These findings, in conjunction with theoretical considerations, suggest that

630 the biochar NH_4^+ adsorption capacity serves as good indicator of the biochar's potential to
631 mitigate NH_3 emissions in aerobic degradation processes. Regarding the linear regression
632 model equation, it appears that increasing the biochar NH_4^+ adsorption capacity by 1
633 $gNNH_4^+.kg^{-1}$ tends to reduce the NH_3 emissions by 2.76% ($gN\text{-}NH_3.gTKNi^{-1}$). Thus, optimizing
634 biochar NH_4^+ adsorption capacity is a promising strategy to increase its capacity to reduce NH_3
635 emissions during aerobic degradation like composting.

636 It is important to note that the linear model presented in Fig. 5 is based on a limited set of
637 controlled experimental conditions and cannot yet be used as a universal predictive tool.
638 Despite this limitation, the results show the potential of the methodology presented in this
639 work. Future researchers interested in further exploring the creation of a predictive test for
640 NH_3 emissions could enhance the dataset presented in this paper. To increase the robustness
641 of this correlation as a predictive tool, it would be advisable to incorporate different organic
642 wastes and biochars made from various substrates, such as straw or bamboo, in future
643 studies.

644 ## 4 Conclusion

645 This study confirmed the existence of a significant and strong correlation between biochar N-
646 NH_4^+ adsorption in a solid organic waste environment and its efficacy in mitigating NH_3
647 emissions during organic waste aerobic degradation processes, such as composting. This
648 correlation shows that biochar $N\text{-}NH_4^+$ adsorption is a good predictor of biochar NH_3
649 emissions reduction during aerobic degradation. This result offers an insight for future studies
650 aiming to develop predictive tools assessing the impact of biochar on the nitrogen cycle in
651 composting. Such tools could assist biochar producers in estimating the potential effects of
652 their products through small-scale, easy-to-execute tests before commercialization, thereby

enhancing the marketability of their products and the trustworthiness of biochar buyers regarding its effects. Furthermore, this research demonstrate that biochar HNO_3 chemical modifications improves biochar capacity to reduce NH_3 emissions during aerobic degradation. Finally, the study demonstrated that certain biochar chemical characteristics, including pH and TO/TC atomic ratio, exhibit strong and significant correlations with biochar $N\text{-}NH_4^+$ adsorption. These attributes were identified as influential factors affecting biochar surface acid groups and electrical properties. The authors recommend that future research seeking to enhance biochar's capacity to reduce NH_3 emissions during composting should prioritize the optimization of its chemical characteristics rather than its physical attributes. Furthermore, to consider an industrial application of these results, a serious economic analysis, including a sustainable price for biochar as highlighted by Marousek et al. (2017), will have to be carried out.

Acknowledgements

This research received a funding from the Regional Council of Bretagne, France.

5 References

Agyarko-Mintah, E., Cowie, Annette, Singh, B.P., Joseph, S., Van Zwieten, L., Cowie, Alan, Harden, S., Smillie, R., 2017. Biochar increases nitrogen retention and lowers greenhouse gas emissions when added to composting poultry litter. Waste Manag. 61, 138–149. https://doi.org/10.1016/j.wasman.2016.11.027

Berthe, L., Druilhe, C., Massiani, C., Tremier, A., de Guardia, A., 2007. Coupling a respirometer and a pycnometer, to study the biodegradability of solid organic wastes during composting. Biosyst. Eng. 97, 75–88. https://doi.org/10.1016/j.biosystemseng.2007.01.013

676 Cáceres, R., Malińska, K., Marfà, O., 2018. Nitrification within composting: A review. Waste Manag.
677 72, 119–137. https://doi.org/10.1016/j.wasman.2017.10.049

678 de Guardia, A., Mallard, P., Teglia, C., Marin, A., Le Pape, C., Launay, M., Benoist, J.C., Petiot, C., 2010.
679 Comparison of five organic wastes regarding their behaviour during composting: Part 1,
680 biodegradability, stabilization kinetics and temperature rise. Waste Manag. 30, 402–414.
681 https://doi.org/10.1016/j.wasman.2009.10.019

682 de Guardia, A., Petiot, C., Rogeau, D., Druilhe, C., 2008. Influence of aeration rate on nitrogen dynamics
683 during composting. Waste Manag. 28, 575–587. https://doi.org/10.1016/j.wasman.2007.02.007

684 Fievet, P., Sbaï, M., Szymczyk, A., Magnenet, C., Labbez, C., Vidonne, A., 2004. A new tangential
685 streaming potential setup for the electrokinetic characterization of tubular membranes. Sep. Sci.
686 Technol. 39, 2931–2949. https://doi.org/10.1081/SS-200028652

687 Gai, X., Wang, H., Liu, J., Zhai, L., Liu, S., Ren, T., Liu, H., 2014. Effects of feedstock and pyrolysis
688 temperature on biochar adsorption of ammonium and nitrate. PLoS One 9, 1–19.
689 https://doi.org/10.1371/journal.pone.0113888

690 Gajalakshmi, S., Abbasi, S.A., 2008. Solid waste management by composting: State of the art, Critical
691 Reviews in Environmental Science and Technology.
692 https://doi.org/10.1080/10643380701413633]

693 Haug, R., 1993. The practical handbook of compost engineering. Lewis Publishers, Boca Raton, Florida

694 Hu, Q., Jung, J., Chen, D., Leong, K., Song, S., Li, F., Mohan, B.C., Yao, Z., Prabhakar, A.K., Lin, X.H., Lim,
695 E.Y., Zhang, L., Souradeep, G., Ok, Y.S., Kua, H.W., Li, S.F.Y., Tan, H.T.W., Dai, Y., Tong, Y.W., Peng,
696 Y., Joseph, S., Wang, C.H., 2021. Biochar industry to circular economy. Sci. Total Environ. 757,
697 143820. https://doi.org/10.1016/j.scitotenv.2020.143820

698 Joseph, S., Kammann, C.I., Shepherd, J.G., Conte, P., Schmidt, H.P., Hagemann, N., Rich, A.M., Marjo,
699 C.E., Allen, J., Munroe, P., Mitchell, D.R.G., Donne, S., Spokas, K., Graber, E.R., 2018.

Microstructural and associated chemical changes during the composting of a high temperature biochar: Mechanisms for nitrate, phosphate and other nutrient retention and release. Sci. Total Environ. 618, 1210–1223. https://doi.org/10.1016/j.scitotenv.2017.09.200

Leip, A., Billen, G., Garnier, J., Grizzetti, B., Lassaletta, L., Reis, S., Simpson, D., Sutton, M.A., De Vries, W., Weiss, F., Westhoek, H., 2015. Impacts of European livestock production: Nitrogen, sulphur, phosphorus and greenhouse gas emissions, land-use, water eutrophication and biodiversity. Environ. Res. Lett. 10. https://doi.org/10.1088/1748-9326/10/11/115004

Li, D., Manu, M.K., Varjani, S., Wong, J.W.C., 2023. Role of tobacco and bamboo biochar on food waste digestate co-composting: Nitrogen conservation, greenhouse gas emissions, and compost quality. Waste Manag. 156, 44–54. https://doi.org/10.1016/j.wasman.2022.10.022

Luxbacher, T., GmbH, A.P., 2014. The zeta potential for solid surface analysis: a practical guide to streaming potential measurement. Anton Paar GmbH, Austria.

Ma, C., Zhao, Y., Chen, H., Liu, Y., Huang, R., Pan, J., 2022. Biochars derived from by-products of microalgae pyrolysis for sorption of gaseous H2S. J. Environ. Chem. Eng. 10, 107370. https://doi.org/10.1016/j.jece.2022.107370

Manu, M.K., Wang, C., Li, D., Varjani, S., Xu, Y., Ladumor, N., Lui, M., Zhou, J., Wong, J.W.C., 2021. Biodegradation kinetics of ammonium enriched food waste digestate compost with biochar amendment. Bioresour. Technol. 341, 125871. https://doi.org/10.1016/j.biortech.2021.125871

Maroušek, J., Vochozka, M., Plachý, J. et al., 2017. Glory and misery of biochar. Clean Techn Environ Policy 19, 311–317. https://doi.org/10.1007/s10098-016-1284-y

Mehmood, S., Ahmed, W., Rizwan, M., Imtiaz, M., Mohamed Ali Elnahal, A.S., Ditta, A., Irshad, S., Ikram, M., Li, W., 2021. Comparative efficacy of raw and HNO3-modified biochar derived from rice straw on vanadium transformation and its uptake by rice (Oryza sativa L.): Insights from photosynthesis, antioxidative response, and gene-expression profile. Environ. Pollut. 289,

117916. https://doi.org/10.1016/j.envpol.2021.117916

Mouhoumed, E.I., Szymczyk, A., Schäfer, A., Paugam, L., La, Y.H., 2014. Physico-chemical characterization of polyamide NF / RO membranes : Insight from streaming current measurements 461, 130–138. https://doi.org/10.1016/j.memsci.2014.03.025

Pardo, G., Moral, R., Aguilera, E., del Prado, A., 2015. Gaseous emissions from management of solid waste: A systematic review. Glob. Chang. Biol. 21, 1313–1327. https://doi.org/10.1111/gcb.12806

Prost, K., Borchard, N., Siemens, J., Kautz, T., Séquaris, J.-M., Möller, A., Amelung, W., 2013. Biochar Affected by Composting with Farmyard Manure. J. Environ. Qual. 42, 164–172. https://doi.org/10.2134/jeq2012.0064

Sanchez-Monedero, M.A., Cayuela, M.L., Roig, A., Jindo, K., Mondini, C., Bolan, N., 2018. Role of biochar as an additive in organic waste composting. Bioresour. Technol. 247, 1155–1164. https://doi.org/10.1016/j.biortech.2017.09.193

Sekar, M., Praveen Kumar, T.R., Selva Ganesh Kumar, M., Vaníčková, R., Maroušek, J., 2021. Techno-economic review on short-term anthropogenic emissions of air pollutants and particulate matter. Fuel 305. https://doi.org/10.1016/j.fuel.2021.121544

Shaaban, A., Se, S.M., Dimin, M.F., Juoi, J.M., Mohd Husin, M.H., Mitan, N.M.M., 2014. Influence of heating temperature and holding time on biochars derived from rubber wood sawdust via slow pyrolysis. J. Anal. Appl. Pyrolysis 107, 31–39. https://doi.org/10.1016/j.jaap.2014.01.021

Shang, L., Xu, H., Huang, S., Zhang, Y., 2018. Adsorption of Ammonium in Aqueous Solutions by the Modified Biochar and its Application as an Effective N-Fertilizer. Water. Air. Soil Pollut. 229. https://doi.org/10.1007/s11270-018-3956-1

747 Song, H., Wang, J., Garg, A., Lin, S., 2020. Exploring mechanism of five chemically treated biochars in
748 adsorbing ammonium from wastewater: understanding role of physiochemical characteristics.
749 Biomass Convers. Biorefinery. https://doi.org/10.1007/s13399-020-01135-9

750 Song, H., Wang, J., Garg, A., Lin, X., Zheng, Q., Sharma, S., 2019. Potential of novel biochars produced
751 from invasive aquatic species outside food chain in removing ammonium nitrogen: Comparison
752 with conventional biochars and clinoptilolite. Sustain. 11, 1–18.
753 https://doi.org/10.3390/su11247136

754 Sujith, S. V, Kim, H., Lee, J., 2022. A Review on Thermophysical Property Assessment of Metal Oxide-
755 Based Nanofluids : Industrial Perspectives 1–21.Steiner, C., Das, K.C., Melear, N., Lakly, D., 2010.
756 Reducing nitrogen loss during poultry litter composting using biochar. J. Environ. Qual. 39, 1236–
757 1242. https://doi.org/10.2134/jeq2009.0337

758 Szymczyk, A., Fatin-Rouge, N., Fievet, P., 2007. Tangential streaming potential as a tool in modeling of
759 ion transport through nanoporous membranes. J. Colloid Interface Sci. 309, 245–252.
760 https://doi.org/10.1016/j.jcis.2007.02.005

761 Szymczyk, A., Fievet, P., Foissy, A., 2002. Electrokinetic characterization of porous plugs from
762 streaming potential coupled with electrical resistance measurements. J. Colloid Interface Sci.
763 255, 323–331. https://doi.org/10.1006/jcis.2002.8591

764 Tag, A.T., Duman, G., Ucar, S., Yanik, J., 2016. Effects of feedstock type and pyrolysis temperature on
765 potential applications of biochar. J. Anal. Appl. Pyrolysis 120, 200–206.
766 https://doi.org/10.1016/j.jaap.2016.05.006

767 Takaya, C.A., Fletcher, L.A., Singh, S., Anyikude, K.U., Ross, A.B., 2016. Phosphate and ammonium
768 sorption capacity of biochar and hydrochar from different wastes. Chemosphere 145, 518–527.
769 https://doi.org/10.1016/j.chemosphere.2015.11.052

770 Tran, H.N., Chao, H.P., You, S.J., 2018. Activated carbons from golden shower upon different chemical

771 activation methods: Synthesis and characterizations. Adsorpt. Sci. Technol. 36, 95–113.
772 https://doi.org/10.1177/0263617416684837

773 Uetani, K., Yano, H., 2012. Zeta Potential Time Dependence Reveals the Swelling Dynamics of Wood
774 Cellulose Nanofibrils 818–827.

775 Vallero, D.A., 2019. Air pollution biogeochemistry, Air Pollution Calculations.
776 https://doi.org/10.1016/b978-0-12-814934-8.00008-9

777 Vieira Firmino, M., Trémier, A., 2023. Nitrogen Losses Mitigation by Supplementing Composting
778 Mixture with Biochar: Research of the Ruling Parameters. Waste and Biomass Valorization.
779 https://doi.org/https://doi.org/10.1007/s12649-023-02204-6

780 Vu, M.T., Chao, H.P., Van Trinh, T., Le, T.T., Lin, C.C., Tran, H.N., 2018. Removal of ammonium from
781 groundwater using NaOH-treated activated carbon derived from corncob wastes: Batch and
782 column experiments. J. Clean. Prod. 180, 560–570.
783 https://doi.org/10.1016/j.jclepro.2018.01.104

784 Vu, T.M., Trinh, V.T., Doan, D.P., Van, H.T., Nguyen, T.V., Vigneswaran, S., Ngo, H.H., 2017. Removing
785 ammonium from water using modified corncob-biochar. Sci. Total Environ. 579, 612–619.
786 https://doi.org/10.1016/j.scitotenv.2016.11.050

787 Wang, Y., Zhang, W., Shang, J., Shen, C., Joseph, S.D., 2019. Chemical aging changed aggregation
788 kinetics and transport of biochar colloids. Environ. Sci. Technol. 53, 8136–8146.
789 https://doi.org/10.1021/acs.est.9b00583

790 Yakout, S.M., 2015. Monitoring the changes of chemical properties of rice straw-derived biochars
791 modified by different oxidizing agents and their adsorptive performance for organics.
792 Bioremediat. J. 19, 171–182. https://doi.org/10.1080/10889868.2015.1029115

793 Yang, H.I., Lou, K., Rajapaksha, A.U., Ok, Y.S., Anyia, A.O., Chang, S.X., 2018. Adsorption of ammonium
794 in aqueous solutions by pine sawdust and wheat straw biochars. Environ. Sci. Pollut. Res. 25,

795 25638–25647. https://doi.org/10.1007/s11356-017-8551-2

796 Yang, W., Shang, J., Li, B., Flury, M., 2020. Surface and colloid properties of biochar and implications
797 for transport in porous media. Crit. Rev. Environ. Sci. Technol. 50, 2484–2522.
798 https://doi.org/10.1080/10643389.2019.1699381

799 Zeng, Y., De Guardia, A., Ziebal, C., De Macedo, F.J., Dabert, P., 2013. Impact of biodegradation of
800 organic matters on ammonia oxidation in compost. Bioresour. Technol. 136, 49–57.
801 https://doi.org/10.1016/j.biortech.2013.02.038

802 Zhang, M., Song, G., Gelardi, D.L., Huang, L., Khan, E., Mašek, O., Parikh, S.J., Ok, Y.S., 2020. Evaluating
803 biochar and its modifications for the removal of ammonium, nitrate, and phosphate in water.
804 Water Res. 186. https://doi.org/10.1016/j.watres.2020.116303

805 Zhao, L., Cao, X., Mašek, O., Zimmerman, A., 2013. Heterogeneity of biochar properties as a function
806 of feedstock sources and production temperatures. J. Hazard. Mater. 256–257, 1–9.
807 https://doi.org/10.1016/j.jhazmat.2013.04.015

808

809 **Table 1.** Physicochemical characterization of substrates

	AW	**OFMSW**	**BC450**	**BC450_HNO3**	**BC450_KOH**	**BC900**	**BC_ C**	**BC_C_HNO$_3$**
Moisture (%)	71.3 (SD = 0.3)	62.4 (SD = 0.6)	5.0 (SD = 0.1)	5.4 (SD = 0.4)	3.1 (SD = 0.2)	5.2 (SD = 0.1)	6.4- 5.9	2.3 (SD = 0.5)
VM (g.kgDM^{-1})	825.4 (SD =3.9)	867.5 (SD = 6.3)	899.7 (SD = 2.2)	971.1 (SD = 1.7)	939.5 (SD = 2.3)	710.0 (SD = 35.9)	918.9 (SD = 18.2)	983.5 (SD = 4.3)
Ashes (g.kgDM^{-1})	171.4 (SD = 1.9)	126.3 (SD = 3.3)	100.2 (SD = 2.2)	28.8 (SD = 1.7)	60.5 (SD = 2.3)	290.0 (SD = 35.9)	81.1 (SD = 18.2)	16.8 (SD = 4.5)
pH (1:5 water to solid ratio w:w)	9.3	8.7	6.7	2.5	5.5	9.9	9.1	3.0
TC (%)	NA	NA	71.74	62.98	72.72	84.08	85.87	76.45

TH (%)	NA	NA	3.65	2.70	3.47	1.14	1.96	1.69
TN (%)	NA	NA	0.65	3.92	0.52	0.26	0.39	1.94
TO (%)	NA	NA	23.96	30.16	20.22	14.56	8.63	16.52
Atomic TO/TC	NA	NA	0.29	0.41	0.24	0.15	0.09	0.19
Specific surface area ($m^2.g^{-1}$)	NA	NA	1.1	1.5	1.26	157.8	74.9	16.9
Easily extractable N-NH_4^+ ($gN\text{-}NH_4.kgDM^{-1}$)	4.1-5.1	5.1-6.9	ND	0.3 (SD < 0.01)	ND	ND	NA	NA
Total N-NH_4^+ ($gN\text{-}NH_4.kgDM^{-1}$)	11.45 (SD = 0.30)	9.16 (SD = 0.35)	NA	NA	NA	NA	NA	NA
TKN ($gN.kgDM^{-1}$)	25.1 (SD = 1.0)	24.4 (SD = 0.4)	4.4 (SD = 0.3)	32.6 (SD = 0.4)	5.1 (SD = 0.1)	2.4 (SD = 0.1)	2.4 (SD = 0.1)	12.7 (SD = 0.2)

Analysis with less than three repetitions had all their values showed in the table.

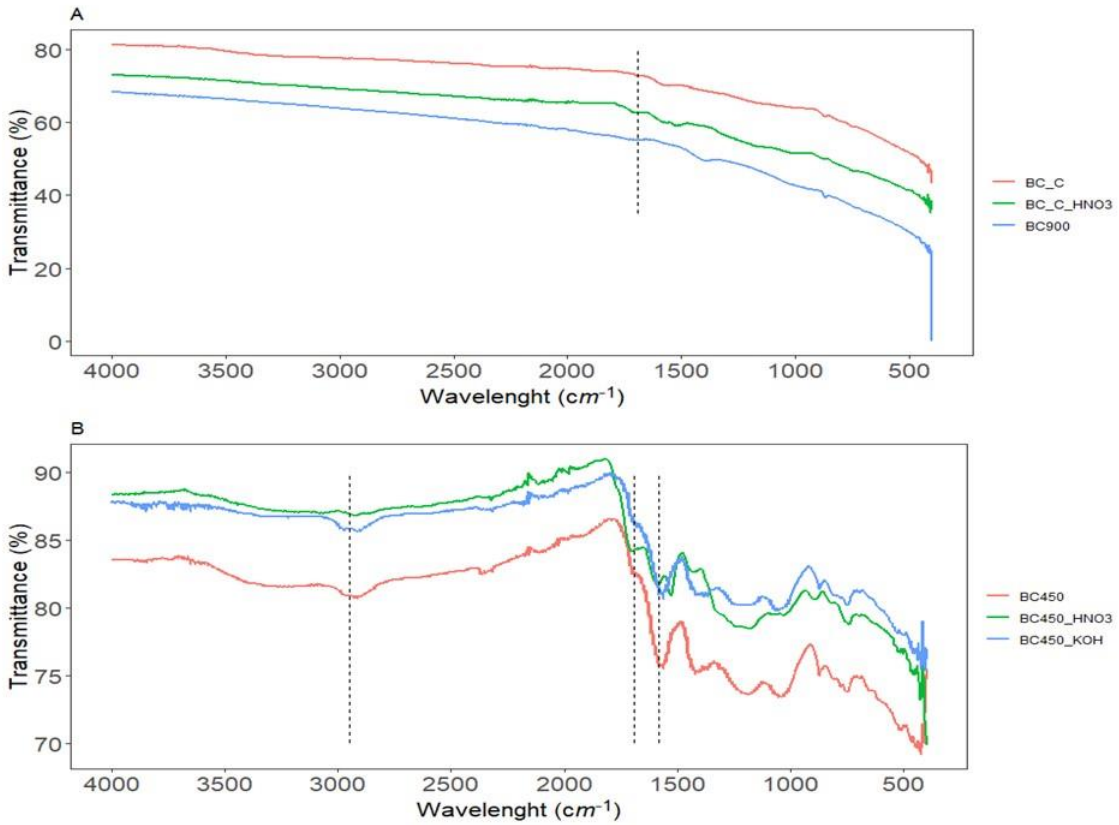

814

815 **Fig. 1.** Fourier transform infrared spectra from (A) BC_C, BC_C_HNO_3 and BC900. (B) BC450, BC450_HNO_3 and BC450_KOH.

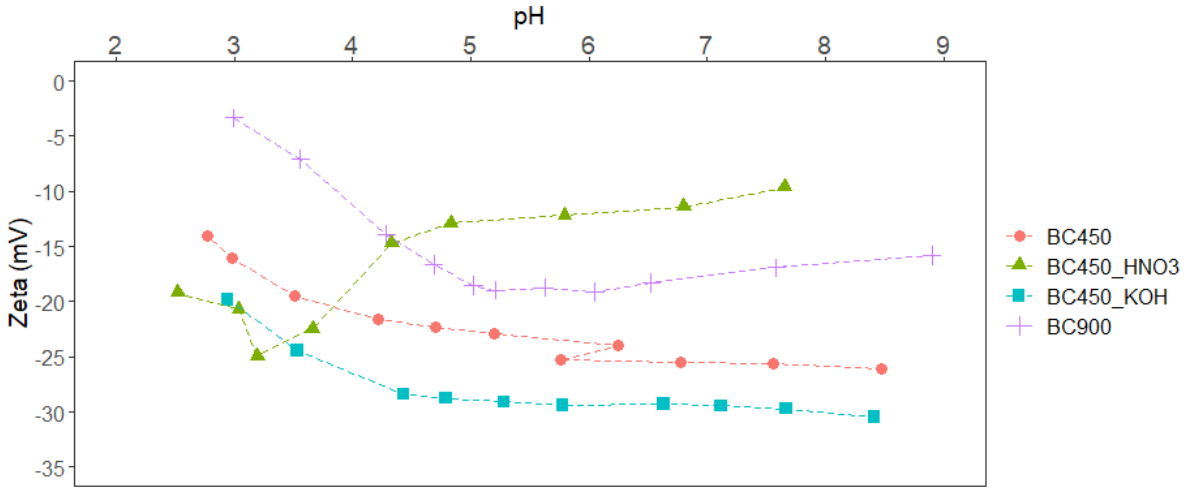

816

817 **Fig. 2.** Zeta potential of BC450, BC450_KOH, BC450_HNO_3 and BC900 inferred from streaming potential measurements vs.

818 pH.

819

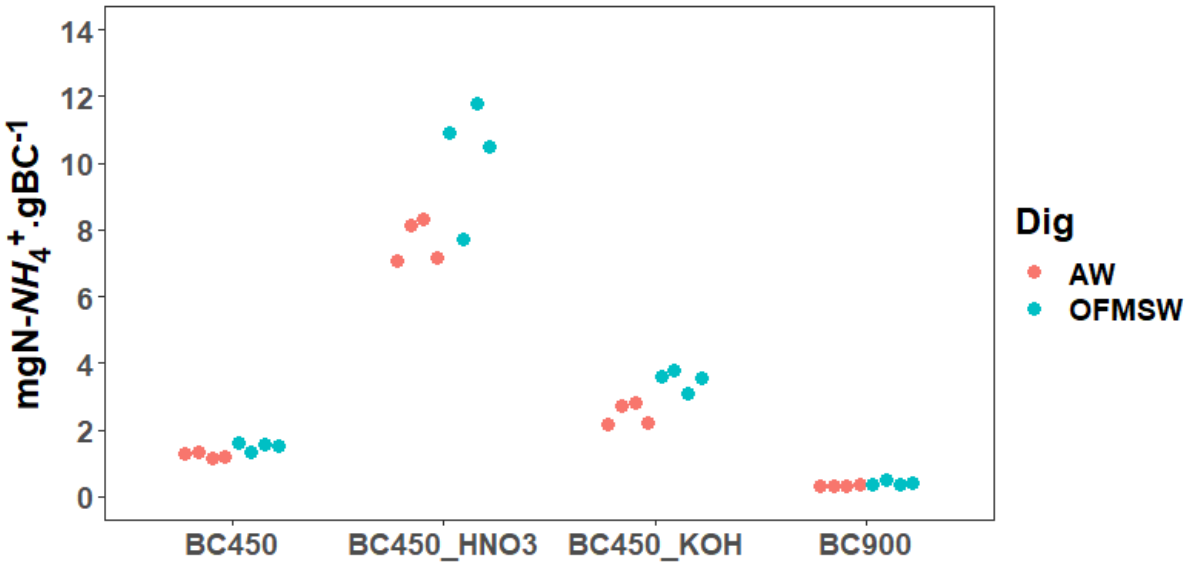

820

821 **Fig. 3.** Ammoniacal nitrogen adsorbed in different biochars when applied to digestate made from agricultural wastes (AW)
822 or digestate made from organic fraction of municipal solid waste (OFMSW).

823

824

825 **Table 2.** Pearson correlation results between NH_3 emissions, biochar N-NH_4^+ adsorption and biochar characteristics

	n	BC pH	TC (%)	TH (%)	TN (%)	TO (%)	Atomic ratio TO/TC	SA ($m^2.g^{-1}$)	DM ($g.kgFM^{-1}$)	VM ($g.kgDM^{-1}$)	Ashes ($g.kgDM^{-1}$)
BC sorp.	4	-0.92*	-0.87	0.19	0.97*	0.86	0.90*	-0.52	0.21	0.71	-0.71

826 BC sorp. = biochar N-NH_4^+ adsorption, n = number of observations, BC = biochar, TC = total carbon, TH = total hydrogen, TN
827 = total nitrogen, TO = total oxygen, elemental analysis expressed as mass percentage in dry weight, SA = surface area, DM =
828 dry matter, FM = fresh matter. '*' represent significant correlations (p-value < 0.1).

829

830 **Table 3.** Aeration rate and oxygen consumption

Experiment	n	Aeration rate mean ($l.h^{-1}$)	Aeration rate SD	Aeration rate CV (%)	Total O_2 consumption ($mmolO2.kgVMi^{-1}$)	Total O_2 consumption SD	Total O_2 consumption CV (%)
Control	3	69.3	2.9	4.2	5.49	0.06	1.1
BC450	3	68.3	4.1	6.0	5.28	0.2	3.78
BC450_KOH	3	68.3	3.4	4.9	5.44	0.07	1.32
BC450_HNO_3	4	69.4	7.0	10.0	5.56	0.05	0.83
BC900	3	71.8	4.4	6.1	5.51	0.23	4.23
BC_C	3	66.3	5.0	7.6	5.42	0.11	1.97
BC_C_HNO3	2	73.5-72.0	NA	NA	5.42-5.58	NA	NA

831 VM_i = initial digestate volatile mater.

832

833 .

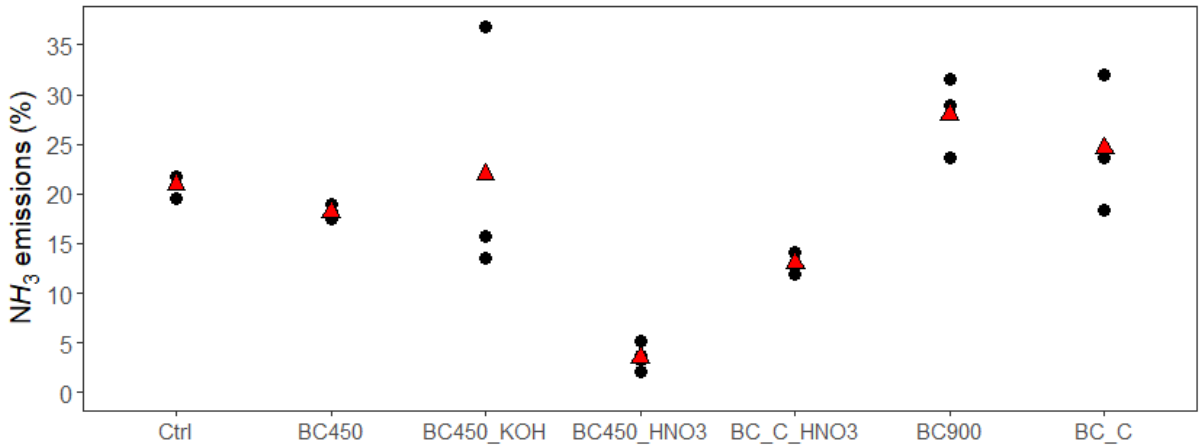

834

835 **Fig. 4.** Ammonia emissions expressed as percentage of Total Kjeldahl Nitrogen. Ctrl = control treatment, without biochar (n
836 = 3), BC450 (n = 3), BC450_KOH (n = 3), BC450_HNO_3 (n = 4), BC_C_HNO_3 (n = 2), BC900 (n = 2), BC_C (n = 3), n = number of
837 observations. Red triangles indicate the treatments means.

838

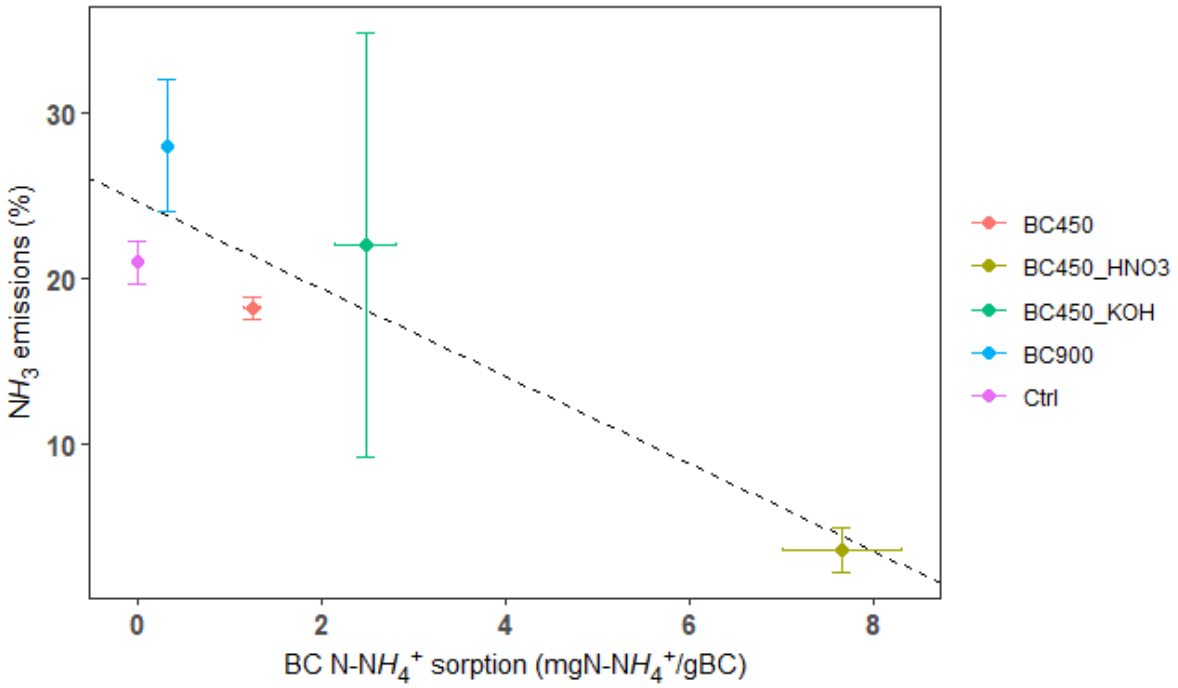

839

840 **Fig. 5.** Linear regression between Biochar ammoniacal nitrogen adsorption and NH_3 emissions during aerobic biodegradation
841 of AW. Vertical and horizontal bars represent the standard errors from NH_3 emissions and BC N-NH_4^+ adsorption,
842 respectively. $NH_{3emissions} = -2.76.BC_{NNH4sorption} + 25.47$, $R^2 = 0.79$, p-value = 0.043. The complete linear regression table can be
843 visualized in the Supplementary Materials.

844